JACS
JOURNAL OF THE AMERICAN CHEMICAL SOCIETY
Article
pubs.acs.org/JACS

Two-Electron Redox Chemistry at the Dinuclear Core of a TePt Platform: Chlorine Photoreductive Elimination and Isolation of a $Te^{V}Pt^{I}$ Complex

Tzu-Pin Lin and François P. Gabbaï*

Department of Chemistry, Texas A&M University, College Station, Texas 77843, United States

Supporting Information

ABSTRACT: As part of our interest in novel redox-active main group/transition metal platforms for energy applications, we have synthesized the chloride salt of $[Te^{III}Pt^{I}Cl(o\text{-dppp})_2]^+$ ($[\mathbf{1}]^+$, *o*-dppp = *o*-$(Ph_2P)C_6H_4$) by reaction of the new bis(phosphino) telluroether $(o\text{-}(Ph_2P)C_6H_4)_2Te$ with $(Et_2S)_2PtCl_2$. Complex $[\mathbf{1}]^+$ is chemically robust and undergoes a clean two-electron oxidation reaction in the presence of $PhICl_2$ to afford $ClTe^{III}Pt^{III}Cl_3(o\text{-dppp})_2$ (**2**), a complex combining a hypervalent four-coordinate tellurium atom and an octahedral platinum center. While the Te−Pt bond length is only slightly affected by the oxidation state of the TePt platform, DFT and NBO calculations show that this central linkage undergoes an umpolung from Te→Pt in $[\mathbf{1}]^+$ to Te←Pt in **2**. This umpolung signals an increase in the electron releasing ability of the tellurium center upon switching from an eight-electron configuration in $[\mathbf{1}]^+$ to a hypervalent configuration in **2**. Remarkably, the two-electron redox chemistry displayed by this new dinuclear platform is reversible as shown by the photoreductive elimination of a Cl_2 equivalent when **2** is irradiated at 350 nm in the presence of a radical trap such as 2,3-dimethyl-1,3-butadiene. This photoreductive elimination, which affords $[\mathbf{1}][Cl]$ with a maximum quantum yield of 4.4%, shows that main group/late transition metal complexes can mimic the behavior of their transition metal-only analogues and, in particular, undergo halogen photoelimination from the oxidized state. A last notable outcome of this study is the isolation and characterization of $F(MeO)_2Te^{V}Pt^{I}Cl(o\text{-dppp})_2$ (**4**), the first metalated hexavalent tellurium compound, which is formed by reaction of **2** with KF in the presence of MeOH.

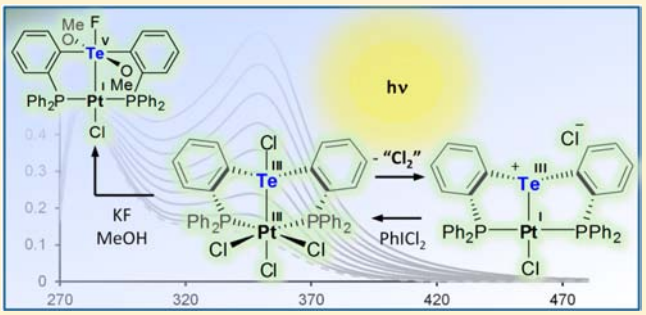

INTRODUCTION

Dinuclear complexes which feature two non-bonded electron-rich elements in close proximity are typically prone to two-electron oxidation reactions.[1] These reactions are facilitated by (i) electron−electron repulsions which destabilize the reduced form and (ii) formation of a covalent element−element bond which stabilizes the oxidized form. This descriptor is general and can be employed to account for the behavior of numerous dinuclear compounds including main group and transition metal derivatives. Examples of such dinuclear main group complexes include dichalcogenide derivatives in which the two group 16 elements are held in close proximity within cyclic structures and/or using rigid linkers.[1a,b] An example of such a compound is 1,5-ditelluracyclooctane (**A**, Chart 1), a compound that undergoes a facile two-electron oxidation reaction with halogen to afford the corresponding $Te^{III}Te^{III}$ ditellurane.[1c,d] Remarkably, these oxidation reactions are chemically reversible as in the case of $[TeI(CH_2)_3]_2$ which undergoes reduction when treated with PhSH.[2] This reversible two-electron redox chemistry bears a strong similarity with that observed for dinuclear late transition metal complexes including A-frame $Au^{I}Au^{I}$ complexes such as $[Au(CH_2)_2PPh_2]_2$ (**B**, Chart 1).[1e] Indeed, analogously to the tellurium systems, these complexes react with halogens to afford $Au^{II}Au^{II}$ complexes.[1f,g] These systems also react with alkyl halides

Chart 1. Two-Electron Redox Processes in Selected Dinuclear Complexes

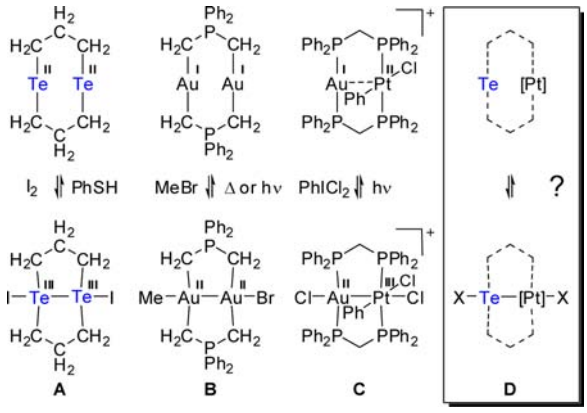

such as MeBr.[1h] In this case, the oxidative addition can be reversed by simple elevation of the temperature or by UV irradiation.

Received: May 11, 2012
Published: June 18, 2012

   dx.doi.org/10.1021/ja3046074 | J. Am. Chem. Soc. 2012, 134, 12230−12238

The reversibility of these reactions and in particular the thermal or light activation of strong metal−halide bond is an important phenomenon because it provides a pathway for the regeneration of the reduced and thus reactive form of the complex. As previously shown, such reduction reactions are also of relevance to the photocatalytic production of H_2 from HX molecules (X = halogen) and dinuclear transition metal catalysts.[3] In the context of this last application, the Nocera group has recently surveyed several complexes and found that X_2 photoelimination reactions can be sustained by a variety of late transition metal binulcear complexes[4] including AuPt complexes (**C**, Chart 1).[5]

Because of the analogy that exists between the redox properties of dinuclear gold and tellurium complexes as illustrated in Chart 1, it occurred to us that heteronuclear complexes combining tellurium and a late transition metal element may also sustain reversible two-electron redox chemistry. In pursuit of this idea, we have decided to explore the synthesis and redox properties of TePt complexes (**D**, Chart 1). In this article, we describe the synthesis and characterization of such complexes. We also show that such complexes display unusual redox properties and in particular support the addition and photoreductive elimination of a X_2 equivalent. Another important aspect of this article is the synthesis and characterization of the first telluroxanyl-metal complex.

RESULTS AND DISCUSSION

Synthesis and Characterization of a $Te^{III}Pt^{I}$ ([1]$^+$) and $Te^{III}Pt^{III}$ Complex (2). We have recently observed that late transition metal complexes featuring the triphosphanylstibine ligand [(*o*-$(Ph_2P)C_6H_4)_3Sb$] are structurally robust and can, in some cases, sustain reversible redox reactions.[6] Encouraged by these observations, we targeted the tellurium analogue, namely [(*o*-$(Ph_2P)C_6H_4)_2Te$], which could be conveniently prepared by treatment of *o*-lithio-diphenylphosphinobenzene with $TeCl_4$. Reaction of [(*o*-$(Ph_2P)C_6H_4)_2Te$] with $(Et_2S)_2PtCl_2$ afforded the cationic complex [**1**]$^+$ as a chloride salt (Scheme 1). This

Scheme 1. Synthesis of [1][Cl] and 2

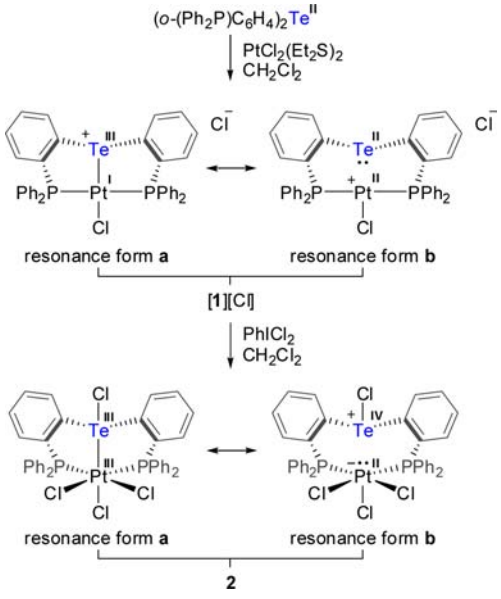

complex gives rise to (i) a ^{31}P NMR signal at 42.5 ppm with ^{195}Pt and ^{125}Te satellites ($^1J_{Pt\text{-}P}$ = 2480 Hz, $J_{Te\text{-}P}$ = 62 Hz) and (ii) a ^{125}Te NMR signal at 1023 ppm split into a triplet ($J_{Te\text{-}P}$ = 62 Hz) and flanked by ^{195}Pt satellites ($^1J_{Te\text{-}Pt}$ = 649 Hz). These spectroscopic features, and in particular the observed P−Pt and Te−Pt coupling, indicate coordination of the tellurium and phosphorus atoms to the platinum center. This coordination mode is confirmed by the crystal structure of this complex which features a platinum center in a distorted square planar geometry (P(1)−Pt−P(2) = 168.19(4)°, Te−Pt−Cl(1) = 175.33(3)°) (Figure 1). The tellurium atom is coordinated to the platinum

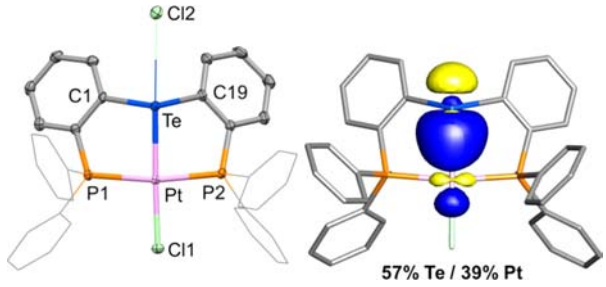

Figure 1. Left: Solid-state structure of [**1**][Cl]. Thermal ellipsoids are drawn at the 50% probability level. Phenyl groups are drawn in wireframe. Hydrogen atoms and solvent molecules are omitted for clarity. Pertinent metrical parameters can be found in the text. Right: NLMO plot (isovalue = 0.05) of the Te−Pt bond in [**1**]$^+$ obtained from NBO analysis. Hydrogen atoms are omitted for clarity.

center via a Te−Pt bond of 2.5281(5) Å which is comparable to the value of 2.5747(6) Å observed in the dicationic complex [Pt{(*o*-$PPh_2C_6H_4$)$TePh$}$_2$]$^{2+}$.[7] A further examination of the structure indicates that the chloride counteranion is weakly interacting with the tellurium center (Te−Cl(2) = 3.1759(12) Å). The Te−Cl(2) separation exceeds the sum of the covalent radii by almost 0.8 Å,[8] leading us to describe this compound as the ion-paired salt [**1**][Cl]. By analogy with formal oxidation state assignments in dinuclear transition metal complexes such as those shown in Chart 1, we describe [**1**]$^+$ on the basis of two resonance structures that correspond to a $Te^{III}Pt^{I}$ and $Te^{II}Pt^{II}$ complex, respectively (resonance forms **a** and **b**, Scheme 1). A consistent formalism is used to describe the other compounds reported in this study.[9]

With this new compound in hand, we decided to investigate its oxidation. Reaction of [**1**][Cl] with $PhICl_2$ afforded complex **2** as a yellow solid. The ^{31}P NMR spectrum of **2** displays a singlet at 26.5 ppm featuring ^{195}Pt and ^{125}Te satellites ($^1J_{Pt\text{-}P}$ = 1777 Hz, $J_{Te\text{-}P}$ = 86 Hz). When compared to [**1**][Cl] ($^1J_{Pt\text{-}P}$ = 2480 Hz), the $^1J_{Pt\text{-}P}$ value of **2** appears to be notably reduced, a phenomenon that is commonly observed for phosphine−platinum complexes upon oxidation.[10] The ^{125}Te NMR signal of **2** at 1217 ppm is split into a triplet by coupling to phosphorus ($J_{Te\text{-}P}$ = 86 Hz). This signal is also coupled to the ^{195}Pt nucleus via a coupling constant ($^1J_{Te\text{-}Pt}$) of 1112 Hz which is larger than that measured for [**1**][Cl] ($^1J_{Te\text{-}Pt}$ = 649 Hz). Since platinum oxidation typically leads to a decrease in coupling constants,[11] we propose that the larger coupling in **2** illustrates a stabilization of the Te−Pt linkage caused by the enhanced donicity of the tellurium atom toward platinum. A final assignment of this structure was derived from a single-crystal X-ray diffraction analysis (Figure 2). While the basic features of the central TePt dinuclear core of **2** including the Te−Pt bond distance (2.6349(7) Å) are analogous to those in [**1**][Cl] (2.5281(5) Å), inspection of the coordination sphere of the platinum center indicates oxidative addition of a Cl_2 molecule, leading to a $Te^{III}Pt^{III}$ complex. As a result, the platinum

dx.doi.org/10.1021/ja3046074 | J. Am. Chem. Soc. 2012, 134, 12230−12238

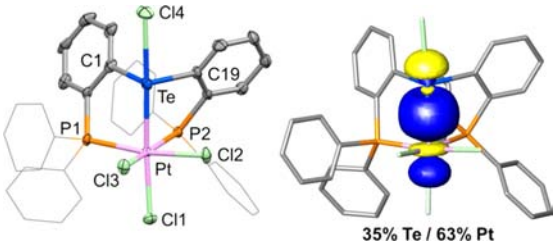

Figure 2. Left: Solid-state structure of **2**. Thermal ellipsoids are drawn at the 50% probability level. Phenyl groups are drawn in wireframe. Hydrogen atoms and solvent molecules are omitted for clarity. Pertinent metrical parameters can be found in the text. Right: NLMO plot (isovalue = 0.05) of the Te−Pt bond in **2** obtained from NBO analysis. Hydrogen atoms are omitted for clarity.

atom adopts an octahedral geometry characteristic of the tetravalent state and with only small angular distortions (Cl(1)−Pt−Te = 171.90(6)°, Cl(2)−Pt−P(1) = 168.26(9)°, Cl(3)−Pt−P(2) = 168.76(8)°). It is interesting to note that the bond distance of 2.451(2) Å separating the platinum atom and the chlorine atom (Cl(1)) *trans* from the tellurium atom is slightly longer than the Pt−Cl bond distances involving the chlorine atoms *trans* from the phosphino ligands (Pt−Cl(2) = 2.396(2) Å and Pt−Cl(3) = 2.388(2) Å). This noticeable difference suggests that the tellurium ligand is a stronger σ-donor than the diphenylphosphino ligands. It could be argued that oxidation only affects the platinum center of this complex. However, changes are also observed in the coordination sphere of the tellurium center with, in particular, a drastic shortening of the Te−Cl(2) bond from 3.1759(12) Å in [**1**][Cl] to 2.712(3) Å in **2**. With this new chlorine ligand in its coordination sphere, the tellurium atom is four-coordinate and adopts a seesaw geometry (Pt−Te−Cl(4) = 178.83(6)° and C(1)−Te−C(19) = 96.4(3)°) reminiscent of that displayed by compounds such as $TePh_2Cl_2$. This analogy is reinforced by the fact that the Te−Cl bond distance in **2** approaches that determined for $TePh_2Cl_2$ (2.51 Å).[12] Thus, complex **2** represents a rare example of a transition metal complex bearing a tetravalent, four-coordinate tellurium atom[13] as opposed to a telluroether ligand.[11,14] The closest analogue of **2** is a complex (**E**) isolated by Puddephat et al. by reaction of Ph_2TeCl_2 with [$PtMe_2$(bu_2bpy)] (bu_2bpy = 4,4′-di-*tert*-butyl-2,2′-bipyridine).[15] This complex features a Pt−Te bond (2.57 Å) of length comparable to that found in **2**. Unlike in **2**, the tellurium center of **E** is best described as three-coordinate, with the chloride ligand forming only a very weak contact of 3.43 Å.

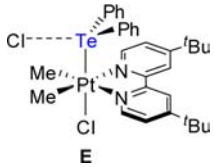

E

To understand how the nature of the Te−Pt bond is affected by oxidation, the structures of [**1**]$^+$ and **2** have also been studied computationally using the Gaussian program[16] (functional, BP86;[17] mixed basis sets: Te/Pt, aug-cc-pVTZ-PP; P/Cl, 6-31g(d); C/H, 6-31g).[18] The resulting structures, which are in excellent agreement with those determined experimentally (see SI), were subjected to a Natural Bond Orbital analysis. This analysis reveals that the Pt−Te bonding pair in [**1**]$^+$ bears a larger orbital contribution from tellurium than platinum (Te, 57%/Pt, 39%), in agreement with the description of the bond as a classical Te→Pt coordination bond. The polarization of the bonding pair in [**1**]$^+$ can be reconciled by considering the partial contribution of a $Te^{II}Pt^{II}$ resonance form (form **b**, Scheme 1) to the electronic structure of the molecule.[9a] By contrast, the bonding pair in **2** features a notably larger orbital contribution from the platinum atom (Te, 35%/Pt, 63%), indicating an umpolung of the Pt−Te bonding pair from Te→Pt in [**1**]$^+$ to Te←Pt in **2**. Such a bond umpolung is not unprecedented and is reminiscent of that observed at the dinuclear core of related AuSb complexes[6] upon oxidation.[19] Additional insights into the electronic structure of **2** can be derived from an inspection of the natural charges (Te 0.93, Pt 0.03 in [**1**]$^+$ and Te 1.23, Pt 0.29 in **2**; see SI) which suggests that oxidation affects both central atoms. These NBO results, including the Pt−Te bond umpolung, indicate that both the $Te^{III}Pt^{III}$ (form **a**, Scheme 1) and $Te^{IV}Pt^{II}$ (form **b**, Scheme 1) resonance forms make important contributions to the electronic structure of **2**. We also note that resonance form **b** corresponds to a telluronium-platinate species in which the telluronium ion is poised to act as a σ-acceptor or Z-ligand.[9b,c,20] The implication of tetravalent tellurium species as Z-ligands is not unprecedented and has been advanced once before in the case of [$(CO)_5$Mn→$TeCl_4$]$^-$, a complex prepared by reaction of the metalloanion [$(CO)_5$Mn]$^-$ with $TeCl_4$.[21]

Photoreductive Elimination of Cl_2 from the $Te^{III}Pt^{III}$ complex 2. As described in the Introduction, the photoactivation of metal−halide bonds is an important process because of its possible implication in catalytic cycles including those for the production of solar fuels.[3] While a significant amount of knowledge has been accumulated for the occurrence of such reactions at the core of transition metal-only bimetallic complexes, dinuclear complexes that combine a main group and transition metal element in their core have never been shown to support such photochemical processes. Bearing in mind that the presence of a main group element at the core of this dinuclear complexes could ultimately result in lower catalyst cost, we decided to determine if **2** could undergo elimination of a Cl_2 equivalent under photolytic conditions. Before testing this hypothesis, the optimized structure of **2** was subjected to a time-dependent density functional theory (TD-DFT) calculation (functional, MPW1PW91; mixed basis set: Te/Pt, aug-cc-pVTZ-PP; P/Cl, 6-31g(d); C/H, 6-31g) using the SMD implicit solvation model with CH_2Cl_2 as a solvent.[22] As shown in Figure 3a, the simulated absorption spectrum nicely matches the experimental one (CH_2Cl_2) thus pointing to the adequacy of this method. As suggested by the TD-DFT calculations, the low energy band centered at 350 nm (25 600 M^{-1} cm^{-1}) originates from electronic transitions from filled orbitals to both LUMO and LUMO+1 (see SI). Examination of these two orbitals (Figure 3b) reveals a set of e_g*-like orbitals which are separated by only 0.003 eV in energy. These orbitals bear significant Te−Cl and Pt−Cl antibonding characters, suggesting that irradiation of the complex at 350 nm may induce chlorine atom dissociation not only from platinum but also possibly from tellurium.

To investigate this possibility, a solution of **2** in CH_2Cl_2 containing 2,3-dimethyl-1,3-butadiene (DMBD) as a radical trap was irradiated with 350 nm light. Such conditions have been previously employed by Nocera and were thus selected to allow for a facile comparison of our results with existing ones.[4] As shown in Figure 4, the absorption band at 350 nm decreases with increasing irradiation times. These spectral changes are assigned to the photochemical conversion of **2** into [**1**][Cl], a phenomenon which is consistent with the ^{31}P NMR observation of [**1**][Cl] as the sole phosphorus-containing species when the

dx.doi.org/10.1021/ja3046074 | J. Am. Chem. Soc. 2012, 134, 12230−12238

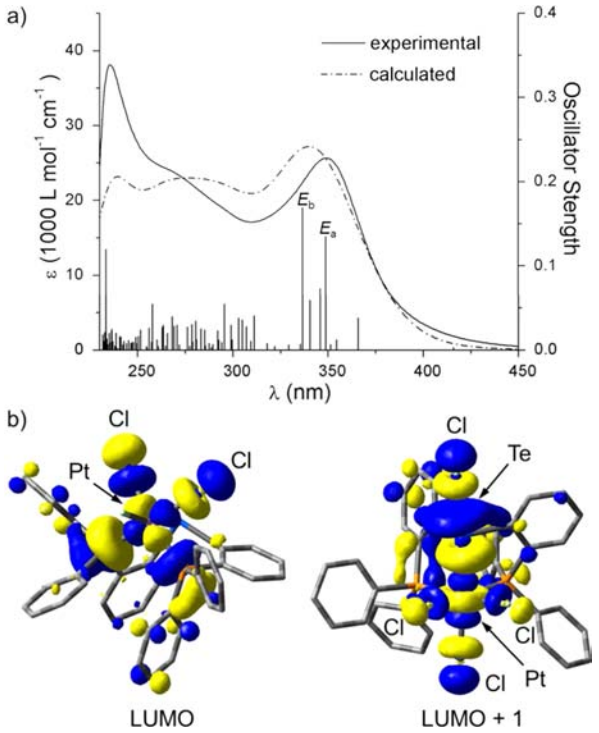

Figure 3. (a) Experimental (CH_2Cl_2) and calculated ultraviolet−visible spectra for **2**. The calculated spectra were obtained by TD-DFT calculations using the MPW1PW91 functional and a mixed basis set (simulated peak half-width = 0.25 eV). In addition to the simulated spectrum, the computed excitations are shown as thin lines with heights proportional to the calculated oscillator strengths. The excitations labeled as E_a and E_b are the main contributors to the low-energy absorption band observed in the absorption spectrum of **2**. A total of 80 singlet excited states were calculated. (b) Plots of the LUMO (−0.092 eV) and LUMO+1 (−0.089 eV) of **2** (at 0.03 isosurface value).

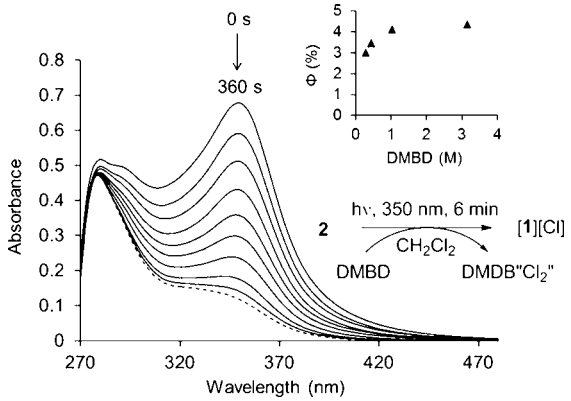

Figure 4. Absorption spectra (—) obtained from the photolysis reaction of 2 in CH_2Cl_2 (2.65×10^{-5} M) with monochromatic 350 nm light in the presence of 2,3-dimethyl-1,3-butadiene (0.29 M). The final spectrum (---) is identical to that of [**1**][Cl]. The inset shows the correlation between the quantum yield and DMBD concentration.

photolysis is carried out in an NMR tube (see SI). GC-MS analysis of the resulting solution also reveals the formation of chlorinated DMBD derivatives referred to as DMBD"Cl_2" (see SI). To assess the efficiency of this photoreduction, quantum yield measurements were carried out. At a DMBD concentration of 0.29 M, a quantum yield of 3.0% can be determined using freshly prepared potassium ferrioxalate as a standard actinometer.[23] This quantum yield moderately increases at higher DMBD concentration to reach a maximum value of 4.4% (at [DMBD] = 3.31 M). The quantum yield measured for the conversion of **2** into [**1**][Cl] is comparable to that measured for the AuPt system (**C**, Chart 1) reported by the Nocera group.[5] The photoreduction of **2** is, however, not as efficient as that of the diplatinum complex $Pt_2(tfepma)_2Cl_6$ (tfepma = $\{(CF_3CH_2O)_2P\}_2NCH_3$) which approaches a quantum efficiency of almost 40% at high DMBD concentrations.[4c] We also note that when **2** is photolyzed in the absence of a radical trap, formation of unidentified photoproducts slowly occurs thus pointing to the chemical vulnerability of the ligand system employed in our study.

The Buffering Role of Tellurium. The umpolung of the Te−Pt bond observed during the conversion of [**1**][Cl] into **2** also signifies a greater extent of σ-donation from the tellurium to the platinum atom upon oxidation. Thus, the tellurium atom acts as an electron reservoir which can alleviate, through increased σ-donation, the electron deficiency caused by oxidative addition of Cl_2. This effect indicates that the two heavy atoms are electronically intimate and operate in a unique synergic fashion. Crucial to the ability of tellurium to donate more extensively to platinum is also the ability of tellurium to accept a chloride anion as an inner sphere ligand *trans* from the platinum atom (Figure 5). Thus, the tellurium atom and its compatibility with a

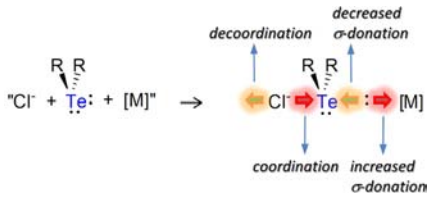

Figure 5. Schematic drawing showing how coordination of a chloride ligand to the tellurium atom serves to modulate the σ-donating properties of the tellurium atom toward the transition metal fragment [M].

hypervalent configuration serves as a relay for a "chloride-push/platinum-pull" effect that allows for a greater degree of electron-pair transfer to the platinum center. The reversibility of the reaction and the photoconversion of **2** into [**1**][Cl] shows that the tellurium atom can step back its donation toward the platinum atom upon photoreduction. Thus, the tellurium atom functions as an electron reservoir that can modulate the electron density of the neighboring platinum atom. We suggest that this buffering effect facilitates, if not enables, the reversibility of the two-electron redox chemistry sustained by this TePt platform.

Reaction of the $Te^{III}Pt^{III}$ Complex 2 with Other Halides: Isolation of a $Te^{V}Pt^{I}$ Complex. Having established that **2** can be efficiently photoreduced, albeit in the presence of a radical trap, we decided to investigate its stability upon exchange of the chloride ligands with other halides. While **2** underwent partial halide exchange when mixed with NaBr in MeOH, we observed the occurrence of a rapid reaction when NaI was employed. This reduction reaction leads to the formation of [**3**][I_3], a salt containing the iodo analogue of [**1**]$^+$ (Scheme 2). Accordingly, the ^{1}H, ^{13}C, ^{31}P, and ^{125}Te NMR spectroscopic features of [**3**]$^+$ are close to those of [**1**]$^+$. We will note, in particular, the similarity of the ^{31}P (42.5 ppm for [**1**]$^+$ vs 37.5 ppm for [**3**]$^+$) and ^{125}Te NMR chemical shifts (1023 ppm for [**1**]$^+$ vs 1018 ppm for [**3**]$^+$) which are also coupled by comparable constants ($^1J_{Te\text{-}Pt}$ = 649 Hz for [**1**]$^+$ vs $^1J_{Te\text{-}Pt}$ = 542 Hz for [**3**]$^+$). The crystal structure of [**3**][I_3] (see SI), confirms its ionic nature, with the [I_3]$^-$ anion

dx.doi.org/10.1021/ja3046074 | J. Am. Chem. Soc. 2012, 134, 12230−12238

Scheme 2. Synthesis of $[3][I_3]$ and 4[a]

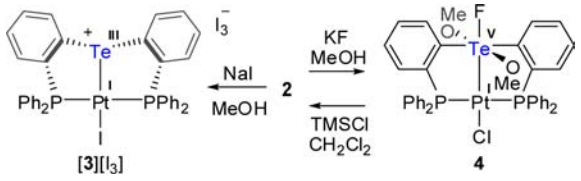

[a]Only one resonance structucture is shown for $[3]^+$. A $Pt^{II}Te^{II}$ resonance form is also relevant.

well separated from $[3]^+$. The structure of the latter is close to that of $[1]^+$ as indicated by the similarities observed in the Te−Pt distances (2.5163(11) Å in $[3]^+$ vs 2.5281(5) Å in $[1]^+$) as well as the Te−Pt−X (173.54(4)° in $[3]^+$ vs 175.33(3)° in $[1]^+$) and P−Pt−P (162.84(14)° in $[3]^+$ vs 168.19(4)° in $[1]^+$) angles. Formation of this compound indicates that iodide can be used to reduce the complex by two electrons, a process also driven by the formation of $[I_3]^-$ anion.

Having tested the behavior of **2** toward bromide and iodide, we turned our attention toward the lighter halide, namely fluoride. Reaction 2 with KF in THF/MeOH (v/v = 8/2) led to the formation of a new compound (**4**) which features a singlet ^{19}F resonance at −58.7 ppm (Figure 6) flanked by a set of ^{125}Te

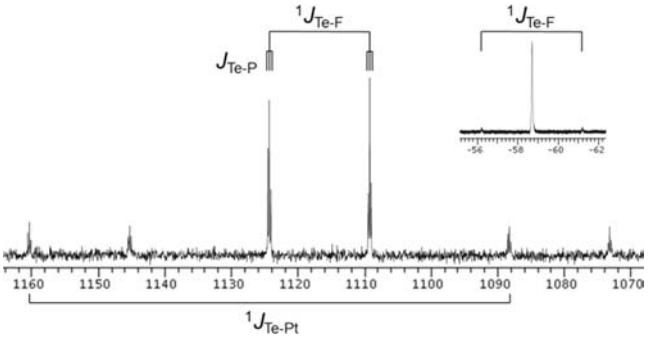

Figure 6. ^{125}Te NMR spectrum of **4** in $CDCl_3$. The inset shows the ^{19}F NMR spectrum.

satellite peaks ($^1J_{Te-F}$ = 1893 Hz). The ^{19}F chemical shift as well as the $^1J_{Te-F}$ coupling constant is comparable to that observed for Ph_5TeF[24] (−42.0 ppm, 1379 Hz) thus pointing to the formation of a tellurium−fluoride bond. This is confirmed by the ^{125}Te resonance of **4** at 1117 ppm which shows coupling of the fluorine nucleus (Figure 6). By analogy with the ^{125}Te NMR chemical shift trend observed in the Ph_nTe series (δ = 727, 509, 467 for n = 2, 4, 6, respectively),[25] the high-valent tellurium nucleus of **4** could have been expected to resonate at high field, when compared to $[1]^+$ (1023 ppm) or **2** (1217 ppm). Bearing in mind that electronegative substituents such as fluorine have a deshielding effect,[26] we speculate that the anomalous chemical shift of **4** results from the balancing of two opposing influences, namely the deshielding induced by the electronegative fluoride and methoxide ligands and the shift to high field typically observed for hexavalent tellurium nucleus. The multiplicity of the ^{125}Te NMR signal also shows coupling of the tellurium nucleus of **4** to two phosphorus nuclei (J_{Te-P} = 48 Hz) as well as to one ^{195}Pt nucleus ($^1J_{Te-Pt}$ = 9044 Hz), thus suggesting an intact PtTe $(o\text{-}Ph_2PC_6H_4)_2$ core. This view is supported by the detection of a single ^{31}P NMR signal at 64.9 ppm coupled to the ^{19}F (J_{F-P} = 6.5 Hz), ^{125}Te (J_{Te-P} = 48 Hz), and ^{195}Pt ($^1J_{Pt-P}$ = 2845 Hz) nuclei. It is important to note that the $^1J_{Te-Pt}$ coupling constant of 9044 Hz measured in **4** is much larger than that observed for $[1][Cl]$ ($^1J_{Te-Pt}$ = 649 Hz) and **2** ($^1J_{Te-Pt}$ = 1112 Hz), a phenomenon that we assign to the greater covalent character of the Pt−Te bond (*vide infra*). Lastly, the ^1H NMR spectrum of **4** features a resonance at 2.77 ppm coupled to ^{19}F ($^4J_{H-F}$ = 1.49 Hz) and ^{125}Te ($^3J_{H-Te}$ = 51.47 Hz) and can be assigned to two tellurium-bound methoxy groups.

The structure of this new derivative was confirmed by a single-crystal X-ray diffraction analysis which shows that **4** is a $Te^{V}Pt^{I}$ complex[9a] featuring a telluroxanyl ligand (Figure 7). The

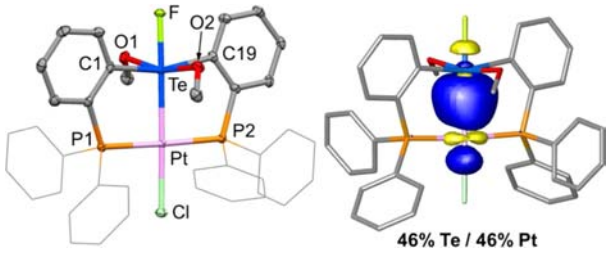

Figure 7. Left: Solid-state structure of **4**. Thermal ellipsoids are drawn at the 50% probability level. Phenyl groups are drawn in wireframe. Hydrogen atoms and solvent molecules are omitted for clarity. Pertinent metrical parameters can be found in the text. Right: NLMO plot (isovalue = 0.05) of the Te−Pt bond in **4** obtained from NBO analysis. Hydrogen atoms are omitted for clarity.

structure of this complex is characterized by (i) a tellurium center in a distorted octahedral geometry as indicated by the Pt−Te−F, O(1)−Te−O(2), and C(1)−Te−C(19) angles of 178.75(6)°, 163.78(11)°, and 165.04(14)°, respectively, and (ii) a platinum center in a square planar geometry as indicated by the Te−Pt−Cl (178.93(3)°) and P(1)−Pt−P(2) (177.81(3)°) angles. The presence of a Te−Pt bond is unambiguously confirmed by a Te-Pt bond distance of 2.5238(5) Å which is almost identical to that in $[1]^+$ (2.5281(5) Å). The short Te−F (1.954(2) Å), Te−O(1) (1.993(3) Å), and Te−O(2) (1.988(2) (2) Å) bonds are comparable to those observed for other hexavalent tellurium species with similar linkages (Te−F = 2.011 (2) Å in Ph_5TeF,[24] Te−O = 1.930(3) and 1.945(4) Å in $(Ph_3SnO)_2Te(OMe)_4$).[27] To our knowledge, compound **4** is the first example of a hexavalent tellurium ligand in the coordination sphere of a metal. Indeed, while telluroether complexes are well known,[11,14] complexes featuring hypervalent tellurium species as ligands are extremely scarce and limited to tetravalent tellurium species.[13,21] According to computations carried out at the same level of theory as for $[1]^+$ and **2** (*vide supra*), platinum and tellurium make a very balanced orbital contribution to the Pt−Te bond (Pt, 46%/Te, 46%) indicative of a dominating covalent character. This situation contrasts with the Te→Pt and Te←Pt bond polarization observed in $[1]^+$ and **2**, respectively.

Conversion of **2** into **4** can be viewed as resulting from an internal two-electron redox reaction in which the platinum center is converting from the formal +III to the +I oxidation state while the tellurium center switches from +III to the +V oxidation state. This internal redox reaction is driven by the preference of tellurium and platinum for hard and soft ligands, respectively. Formation of **4** as a bis(methoxy) derivative is serendipitous since the reaction was carried out with an excess of NaF. Presumably, the weakly basic fluoride anion promotes deprotonation of the methanol solvent, leading to complex **4** as a monofluorobis(methoxide)- rather than a trifluoro-tellurium species. The strength of the hexavalent tellurium oxygen or

dx.doi.org/10.1021/ja3046074 | J. Am. Chem. Soc. 2012, 134, 12230−12238

fluorine bond is reflected by the stability of **4** to UV irradiation. Formation of **4** is, however, chemically reversible. Indeed, **4** reacts with trimethylsilyl chloride (TMSCl) to produce **2** as well as TMSF and TMSOMe, two silyl products that are readily detected by NMR spectroscopy (see SI). When the reaction is carried out on a preparative scale, **2** can be recovered in 82% yield (Scheme 2).

CONCLUSION

In summary, we report that the $Te^{III}Pt^{I}$ coordination complex $[\mathbf{1}]^+$ is readily oxidized by a Cl_2 equivalent to afford the corresponding $Te^{III}Pt^{III}$ complex **2**. This oxidative addition reaction can be reversed by simple UV irradiation in the presence of a radical trap. By uncovering these new reversible two-electron redox reactions, we show, for the first time, that main group/late transition metal complexes can mimic the behavior of their transition metal-only analogues and, in particular, undergo halogen photoelimination from the oxidized state. A unique facet of this new redox-active TePt platform originates from the capacity of the tellurium atom to buffer the electron density of the redox-active platinum center. These buffering properties are made possible by the ability of the tetravalent tellurium center to switch between a regular eight-electron and hypervalent configuration. These effects and their impact on the reversibility of the two-electron chemistry displayed by this new platform are not only of fundamental importance but may also be of relevance to the field of HX splitting photocatalysis. Finally, we describe that compound **2** undergoes an internal two-electron redox reaction in the presence of hard anions to afford complex **4**, the first metalated hexavalent tellurium compound.

EXPERIMENTAL SECTION

General Considerations. *cis*-$PtCl_2(Et_2S)_2$[28] and $PhICl_2$[29] were prepared according to the reported procedures. Solvents were dried by passing through an alumina column (*n*-pentane and CH_2Cl_2) or by reflux under N_2 over Na/K (Et_2O and THF). All other solvents were used as received. $TeCl_4$, NaI, KF, and TMSCl were purchased from Aldrich and used as received. Ambient temperature NMR spectra were recorded on a Varian Unity Inova 400 FT NMR (399.59 MHz for ^1H, 100.45 MHz for ^{13}C, 375.89 MHz for ^{19}F, 161.74 MHz for ^{31}P, 126.14 MHz for ^{125}Te) spectrometer. Chemical shifts (δ) are given in ppm and are referenced against residual solvent signals (^1H, ^{13}C) or external $BF_3{-}Et_2O$ (^{19}F), H_3PO_4 (^{31}P), and Ph_2Te_2 (^{125}Te). Elemental analyses were performed at Atlantic Microlab (Norcross, GA). Electrospray mass spectra were obtained with a SciexQstarr Pulsar and a Protana Nanospray ion source.

Synthesis of [(*o*-$(Ph_2P)C_6H_4)_2$Te]. To an Et_2O solution (5 mL) of *o*-$(Ph_2P)C_6H_4Br$ (0.81 g, 2.374 mmol) was added a *n*-hexane solution of *n*-BuLi (2.87 M, 0.99 mL, 2.849 mmol) at ambient temperature. The mixture was stirred for 20 min, resulting in the precipitation of *o*-$(Ph_2P)C_6H_4Li$. This lithium salt was washed with Et_2O (3 × 5 mL) and suspended in an Et_2O solution (3 mL). To this suspension was added a THF solution (3 mL) of $TeCl_4$ (160 mg, 0.594 mmol) dropwise at ambient temperature. After stirring for 12 h, the solvent was removed under reduced pressure to afford a brown solid. The product was re-dissolved in CH_2Cl_2 (30 mL) and filtered through Celite. Removal of CH_2Cl_2 under reduced pressure afforded $[(o\text{-}(Ph_2P)C_6H_4)_2Te]$ as a light yellow solid which was washed with Et_2O (3 × 5 mL) and *n*-pentane (3 × 5 mL) and dried under vacuum (169 mg, 43.8% yield based on $TeCl_4$). ^1H NMR (399.59 MHz; $CDCl_3$): δ 6.85 (d, 2H, *o*-P(Te)C_6H_4, $^3J_{H\text{-}H}$ = 7.63 Hz), 6.98 (pseudo t, 2H, *m*-P(Te)C_6H_4, $^3J_{H\text{-}H}$ = 7.63 Hz), 7.09 (pseudo t, 2H, *m*-P(Te)C_6H_4, $^3J_{H\text{-}H}$ = 7.63 Hz), 7.16−7.29 (m, 20H), 7.39 (d, 2H, *o*-P(Te)C_6H_4, $^3J_{H\text{-}H}$ = 7.63 Hz). $^{13}C\{^1H\}$ NMR (100.45 MHz; $CDCl_3$): δ 128.0 (s), 128.5 (d, $J_{C\text{-}P}$ = 6.87 Hz), 128.6 (s), 129.9 (s), 133.5 (s), 133.8 (d, $J_{C\text{-}P}$ = 19.45 Hz), 134.1 (s), 137.0 (d, $J_{C\text{-}P}$ = 11.00 Hz), 138.5 (d, $J_{C\text{-}P}$ = 8.40 Hz), 143.4 (d, $J_{C\text{-}P}$ = 3.77 Hz). $^{31}P\{^1H\}$ NMR (161.74 MHz; $CDCl_3$): δ -0.3 (s, $J_{Te\text{-}P}$ = 416 Hz). $^{125}Te\{^1H\}$ NMR (126.14 MHz; $CDCl_3$): δ 580 (t, $J_{Te\text{-}P}$ = 416 Hz).

Synthesis of [1][Cl]. A solution of $PtCl_2(Et_2S)_2$ (27.5 mg, 0.062 mmol) in CH_2Cl_2 (2 mL) was added to a solution of $[(o\text{-}(Ph_2P)C_6H_4)_2Te]$ (40 mg, 0.062 mmol) in CH_2Cl_2 (5 mL) at ambient temperature. The resulting clear yellow solution was stirred for 12 h and evacuated to dryness under reduced pressure. The resulting residue was washed with Et_2O (3 × 5 mL) to afford a pure sample of $[\mathbf{1}][Cl]$ as a light yellow crystalline solid (55 mg, 97.4% yield). Yellow crystals of $[\mathbf{1}][Cl]{-}CH_2Cl_2$ suitable for X-ray diffraction analysis were obtained by diffusion of Et_2O into a CH_2Cl_2 solution of $[\mathbf{1}][Cl]$. ^1H NMR (499.42 MHz; $CDCl_3$): δ 7.09 (d of t, 2H, *o*-P(Te)C_6H_4, $^3J_{H\text{-}H}$ = 7.28 Hz, $^3J_{H\text{-}P}$ = 4.49 Hz), 7.35−7.45 (m, 8H), 7.49−7.59 (m, 10H), 7.61-7.66 (m, 4H), 7.72 (pseudo t, 2H, *m*-P(Te)C_6H_4, $^3J_{H\text{-}H}$ = 7.33 Hz), 9.38 (d, 2H, *o*-P(Te)C_6H_4, $^3J_{H\text{-}H}$ = 8.04 Hz). $^{13}C\{^1H\}$ NMR (125.58 MHz; $CDCl_3$): δ 127.0 (t, $J_{C\text{-}P}$ = 31.74 Hz), 128.6 (t, $J_{C\text{-}P}$ = 5.73 Hz), 129.7 (t, $J_{C\text{-}P}$ = 5.73 Hz), 131.3 (t, $J_{C\text{-}P}$ = 3.71 Hz), 132.2 (d, $J_{C\text{-}P}$ = 60.86 Hz), 133.7−133.9 (m, 2C), 135.8 (s), 137.3 (t, $J_{C\text{-}P}$ = 6.76 Hz), 142.0 (t, $J_{C\text{-}P}$ = 31.84 Hz). $^{31}P\{^1H\}$ NMR (161.74 MHz; $CDCl_3$): δ 42.5 (s, $J_{Te\text{-}P}$ = 62 Hz, $J_{Pt\text{-}P}$ = 2480 Hz). $^{125}Te\{^1H\}$ NMR (126.14 MHz; $CDCl_3$): δ 1023 (t, $J_{Te\text{-}P}$ = 62 Hz, $^1J_{Te\text{-}Pt}$ = 649 Hz). The ^{195}Pt NMR resonance of this compound could not be detected. Elemental analysis calculated (%) for $[\mathbf{1}][Cl]{-}CH_2Cl_2$ ($C_{36}H_{28}Cl_2P_2PtTe + CH_2Cl_2$): C, 44.39; H, 3.02; found C, 44.31; H, 3.13.

Synthesis of 2. A solution of $[\mathbf{1}][Cl]$ (80 mg, 0.087 mmol) in CH_2Cl_2 (2 mL) was added to a solution of $PhICl_2$ (26 mg, 0.087 mmol) in $CHCl_3$ (2 mL) at ambient temperature. A yellow precipitate was formed immediately. After the mixture was stirred for 2 h, 10 mL of Et_2O was added. The resulting yellow precipitate was collected by filtration and dried under vacuum, to afford **2** (81 mg, 94.0% yield). Compound **2**, whose chemical composition has been established by HRMS and elemental analysis (see below), has low solubility in organic solvent. The NMR spectra of **2** was recorded from a *in situ* reaction of $[\mathbf{1}][Cl]$ (15 mg, 0.016 mmol) with $PhICl_2$ (4.5 mg, 0.016 mmol) in $CDCl_3$. Yellow crystals of **2**-THF suitable for X-ray diffraction analysis were obtained from diffusing Et_2O into a THF solution of **2**. ^1H NMR (499.42 MHz; $CDCl_3$): δ 7.11 (t, 2H, *m*-P(Te)C_6H_4, $^3J_{H\text{-}H}$ = 7.61 Hz), 7.31−7.77 (m, 20H), 8.10−8.15 (m, 4H), 9.23 (d, 2H, *o*-P(Te)C_6H_4, $^3J_{H\text{-}H}$ = 8.08 Hz). A satisfactory $^{13}C\{^1H\}$ NMR spectrum could not be recorded due to precipitation. $^{31}P\{^1H\}$ NMR (161.74 MHz; $CDCl_3$): δ 26.5 (s, $J_{Te\text{-}P}$ = 86 Hz, $J_{Pt\text{-}P}$ = 1777 Hz). $^{125}Te\{^1H\}$ NMR (126.14 MHz; $CDCl_3$): δ 1217 (t, $J_{Te\text{-}P}$ = 86 Hz, $^1J_{Te\text{-}Pt}$ = 1112 Hz). The ^{195}Pt NMR resonance of this compound could not be detected. HRMS (ESI^+) calcd for $[M{-}Cl]^+$ ($C_{36}H_{28}Cl_3P_2PtTe^+$): 950.9495, found: 950.9479. Elemental analysis calculated (%) for **2** ($C_{36}H_{28}Cl_4P_2PtTe$): C, 43.81; H, 2.86; found C, 43.52; H, 2.94.

Reaction of 2 with NaBr. A sample of **2** dissolved in d_4-MeOH was mixed with an excess of NaBr in an NMR tube. Analysis of the reaction mixture by ^1H and ^{31}P NMR spectroscopy after 2 and 12 h did not show any changes. ESI MS analysis

dx.doi.org/10.1021/ja3046074 | J. Am. Chem. Soc. 2012, 134, 12230−12238

of the mixture showed peaks suggesting the possible formation of mixed chloride/bromide species.

Synthesis of [3][I_3]. To a THF (5 mL) solution of **2** (79 mg, 0.080 mmol) was added a MeOH (5 mL) solution of NaI (60 mg, 0.400 mmol) at ambient temperature. The mixture turned from a yellow suspension to dark purple solution immediately. After stirring for 30 min, the solvent was removed under reduced pressure. The product was re-dissolved in CH_2Cl_2 (10 mL), and the insoluble white precipitate was filtered off by passing through a short plug of Celite. The solvent was then removed under reduced pressure to give a purple crystalline solid which was washed with with Et_2O (3 × 5 mL) and dried under vacuum to afford a pure sample of [1-I][I_3] (90 mg, 83.1% yield). Purple needle crystals of [**3**][I_3]−CH_2Cl_2 suitable for X-ray diffraction analysis were obtained by diffusion of Et_2O into a CH_2Cl_2 solution of [**3**][I_3]. ^{1}H NMR (499.42 MHz; $CDCl_3$): δ 7.08 (d of t, 2H, *o*-P(Te)C_6H_4, $^3J_{H\text{-}H}$ = 7.28 Hz, $^3J_{H\text{-}P}$ = 4.49 Hz), 7.29−7.34 (m, 4H), 7.44−7.53 (m, 6H), 7.58−7.62 (m, 8H), 7.67−7.73 (m, 4H), 7.84 (pseudo t, 2H, *m*-P(Te)C_6H_4, $^3J_{H\text{-}H}$ = 7.97 Hz), 8.70 (d, 2H, *o*-P(Te)C_6H_4, $^3J_{H\text{-}H}$ = 7.94 Hz). ^{13}C{^{1}H} NMR (125.58 MHz; $CDCl_3$): δ 127.3 (t, $J_{C\text{-}P}$ = 27.85 Hz), 128.5 (t, $J_{C\text{-}P}$ = 5.63 Hz), 130.1 (t, $J_{C\text{-}P}$ = 5.63 Hz), 131.8 (t, $J_{C\text{-}P}$ = 3.90 Hz), 132.5 (d, $J_{C\text{-}P}$ = 87.83 Hz), 134.0 (t, $J_{C\text{-}P}$ = 5.98 Hz), 134.1 (t, $J_{C\text{-}P}$ = 7.26 Hz), 134.5 (s), 136.8 (t, $J_{C\text{-}P}$ = 7.60 Hz), 137.7 (t, $J_{C\text{-}P}$ = 3.09 Hz). ^{31}P{^{1}H} NMR (161.74 MHz; $CDCl_3$): δ 37.5 (s, $J_{Te\text{-}P}$ = 49 Hz, $J_{Pt\text{-}P}$ = 2336 Hz). ^{125}Te{^{1}H} NMR (126.14 MHz; $CDCl_3$): δ 1018 (t, $J_{Te\text{-}P}$ = 49 Hz, $^1J_{Te\text{-}Pt}$ = 542 Hz). The ^{195}Pt NMR resonance of this compound could not be detected. Elemental analysis calculated (%) for [**3**][I_3] ($C_{36}H_{28}I_4P_2PtTe$): C, 31.96; H, 2.09; found C, 31.86; H, 2.14.

Synthesis of 4. To a THF (8 mL) solution of **2** (150 mg, 0.152 mmol) was added a MeOH (2 mL) solution of KF (44.1 mg, 0.760 mmol) at ambient temperature. The mixture turned from a yellow suspension to a colorless suspension over 5 min. After stirring for 2 h, the solvent was removed under reduced pressure. The product was re-dissolved in CH_2Cl_2 (10 mL), and the insoluble white precipitate was filtered off by passing through a short plug of Celite. The solvent was again removed under reduced pressure to give a white solid which was washed with Et_2O (3 × 5 mL) and dried under vacuum to afford a pure sample of **3** (105 mg, 71.8% yield). Colorless crystals of **4** suitable for X-ray diffraction analysis were obtained by diffusion of Et_2O into a CH_2Cl_2 solution of **4**. ^{1}H NMR (499.42 MHz; $CDCl_3$): δ 2.77 (d, 6H, OMe, $^4J_{H\text{-}F}$ = 1.49 Hz, $^3J_{H\text{-}Te}$ = 51.47 Hz), 7.37−7.48 (m, 16H), 7.57−7.62 (m, 10H), 8.71 (d, 2H, *o*-P(Te)C_6H_4, $^3J_{H\text{-}H}$ = 7.65 Hz, $^3J_{H\text{-}Te}$ = 44.60 Hz). ^{13}C{^{1}H} NMR (125.58 MHz; $CDCl_3$): δ 52.4 (s, OMe), 124.3 (t, $J_{C\text{-}P}$ = 30.39 Hz), 128.5 (t, $J_{C\text{-}P}$ = 5,61 Hz), 129.3 (t, $J_{C\text{-}P}$ = 29.05 Hz), 130.4 (t, $J_{C\text{-}P}$ = 3.06 Hz), 131.0 (s), 132.3 (s), 133.3 (d, $J_{C\text{-}P}$ = 2.97 Hz), 133.9 (t, $J_{C\text{-}P}$ = 6.28 Hz), 134.1 (t, $J_{C\text{-}P}$ = 7.84 Hz), 164.2 (d of t, $J_{C\text{-}P}$ = 57.47 Hz, $J_{C\text{-}P}$ = 17.88 Hz). ^{19}F{^{1}H} NMR (375.89 MHz; $CDCl_3$): δ -58.7 (s, $^1J_{Te\text{-}F}$ = 1893 Hz). ^{31}P{^{1}H} NMR (161.74 MHz; $CDCl_3$): δ 64.9 (d, $J_{F\text{-}P}$ = 6.5 Hz, $J_{Te\text{-}P}$ = 48 Hz, $J_{Pt\text{-}P}$ = 2845 Hz). ^{125}Te{^{1}H} NMR (126.14 MHz; $CDCl_3$): δ 1117 (d of t, $^1J_{Te\text{-}F}$ = 1893 Hz, $J_{Te\text{-}P}$ = 48 Hz, $^1J_{Te\text{-}Pt}$ = 9044 Hz). The ^{195}Pt NMR resonance of this compound could not be detected. Elemental analysis calculated (%) for **3** ($C_{38}H_{34}ClFO_2P_2Te$): C, 47.46; H, 3.56; found C, 46.31; H, 3.11.

Computational Details. Density functional theory (DFT) structural optimizations were performed on the solid-state structures of complexes [**1**]$^+$, **2**, and **4** using Gaussian 09 suite of programs with effective core potentials on all heavy atoms (functional, BP86;[17] mixed basis set: Te/Pt, aug-cc-pVTZ-PP; P/Cl, 6-31g(d); F/O, 6-31g(d′); C/H, 6-31g).[18] The optimized structures, which are in excellent agreement with the solid-state structures (see SI), were subjected to a NBO analysis.[30] The resulting Natural Localized Molecular Orbitals (NLMOs) were visualized and plotted in Jimp 2 program.[31] In addition, the optimized structure of **2** was subjected to time-dependent density functional theory (TD-DFT) calculations (functional, MPW1PW91; mixed basis set: Te/Pt, aug-cc-pVTZ-PP; P/Cl, 6-31g(d); C/H, 6-31g) using the SMD implicit solvation model with CH_2Cl_2 as a solvent.[22]

Crystallographic Measurements. The crystallographic measurements were performed at 110(2) K using a Bruker APEX-II CCD area detector diffractometer (Mo Kα radiation, λ = 0.71069 Å). In each case, a specimen of suitable size and quality was selected and mounted onto a nylon loop. The structures were solved by direct methods, which successfully located most of the nonhydrogen atoms. Semi-empirical absorption corrections were applied. Subsequent refinement on F^2 using the SHELXTL/PC package (version 6.1) allowed location of the remaining non-hydrogen atoms.

UV−Vis Absorption Measurements. UV−vis spectra were recorded at room temperature on an Ocean Optics USB4000 spectrometer with an Ocean Optics ISS light source.

Photolysis Reactions and Quantum Yield Measurements. Photolysis reactions were performed using 350 nm light generated from a 75 W xenon lamp with a PTI model 101 monochromator integrated in a PTI QuantaMaster 40 fluorescence spectrometer. Potassium ferrioxalate was freshly prepared as a standard actinometer to determine the photon flux.[23] For details of the quantum yield measurements, see SI.

Gas Chromatography−Mass Spectrometry. GC-MS was performed on Ultra GC/DSQ (ThermoElectron, Waltham, MA). Rxi-5ms was used as a gas chromatographic column with dimensions of 60 m length, 0.25 mm i.d., and 0.25 μm film thickness (Restek, Bellefonte, PA). Helium was used as a carrier gas at constant flow of 1.5 mL/min. Splitless and split (1:10) injection were used. Transfer line and ion source were held at 250 °C. The column temperature was maintained at 50 °C for 5 min and raised to 320 °C at 20 °C/min. Mass spectra were acquired in full scan mode in the range of 30-500 m/z. For details of DMBD"Cl_2" analysis, please see SI.

■ ASSOCIATED CONTENT

Ⓢ Supporting Information

Additional experimental and computational details; crystallographic data in CIF format. This material is available free of charge via the Internet at http://pubs.acs.org.

■ AUTHOR INFORMATION

Corresponding Author

francois@tamu.edu

Notes

The authors declare no competing financial interest.

■ ACKNOWLEDGMENTS

This work was supported by the National Science Foundation (CHE-0952912), the Welch Foundation (A-1423), and Texas A&M University (Davidson Professorship). We also acknowledge Dr. Yohannes Rezenom for the analysis of DMBD"Cl_2" derivatives.

REFERENCES

(1) (a) Evans, D. H.; Gruhn, N. E.; Jin, J.; Li, B.; Lorance, E.; Okumura, N.; Macías-Ruvalcaba, N. A.; Zakai, U. I.; Zhang, S.-Z.; Block, E.; Glass, R. S. *J. Org. Chem.* **2010**, *75*, 1997−2009. (b) Nakayama, N.; Takahashi, O.; Kikuchi, O.; Furukawa, N. *Heteroat. Chem* **2000**, *11*, 31−41. (c) Fujihara, H.; Takaguchi, Y.; Ninoi, T.; Erata, T.; Furukawa, N. *J. Chem. Soc., Perkin Trans. 1* **1992**, 2583−2584. (d) Fujihara, H.; Ninoi, T.; Akaishi, R.; Erata, T.; Furukawa, N. *Tetrahedron Lett.* **1991**, *32*, 4537−4540. (e) Fackler, J. P.; Murray, H. H.; Basil, J. D. *Organometallics* **1984**, *3*, 821−823. (f) Fackler, J. P. *Inorg. Chem.* **2002**, *41*, 6959−6972. (g) Mazany, A. M.; Fackler, J. P. *J. Am. Chem. Soc.* **1984**, *106*, 801−802. (h) Basil, J. D.; Murray, H. H.; Fackler, J. P.; Tocher, J.; Mazany, A. M.; Trzcinska-Bancroft, B.; Knachel, H.; Dudis, D.; Delord, T. J.; Marler, D. *J. Am. Chem. Soc.* **1985**, *107*, 6908−6915.

(2) Two-electron redox chemistry is also well precedented for mononulcear tellurium derivatives. For examples, see: (a) Detty, M. R.; Zhou, F.; Friedman, A. E. *J. Am. Chem. Soc.* **1996**, *118*, 313−318. (b) You, Y.; Ahsan, K.; Detty, M. R. *J. Am. Chem. Soc.* **2003**, *125*, 4918−4927.

(3) (a) Mann, K. R.; Lewis, N. S.; Miskowski, V. M.; Erwin, D. K.; Hammond, G. S.; Gray, H. B. *J. Am. Chem. Soc.* **1977**, *99*, 5525−5526. (b) Mann, K. R.; Bell, R. A.; Gray, H. B. *Inorg. Chem.* **1979**, *18*, 2671−2673. (c) Maverick, A. W.; Gray, H. B. *Pure Appl. Chem.* **1980**, *52*, 2339−2348. (d) Sigal, I. S.; Mann, K. R.; Gray, H. B. *J. Am. Chem. Soc.* **1980**, *102*, 7252−7256. (e) Mann, K. R.; Dipierro, M. J.; Gill, T. P. *J. Am. Chem. Soc.* **1980**, *102*, 3965−3967. (f) Gray, H. B.; Maverick, A. W. *Science* **1981**, *214*, 1201−1205. (g) Eidem, P. K.; Maverick, A. W.; Gray, H. B. *Inorg. Chim. Acta* **1981**, *50*, 59−64. (h) Esswein, A. J.; Nocera, D. G. *Chem. Rev.* **2007**, *107*, 4022−4047. (i) Heyduk, A. F.; Nocera, D. G. *Science* **2001**, *293*, 1639−1641.

(4) (a) Heyduk, A. F.; Macintosh, A. M.; Nocera, D. G. *J. Am. Chem. Soc.* **1999**, *121*, 5023−5032. (b) Teets, T. S.; Nocera, D. G. *J. Am. Chem. Soc.* **2009**, *131*, 7411−7420. (c) Cook, T. R.; Surendranath, Y.; Nocera, D. G. *J. Am. Chem. Soc.* **2009**, *131*, 28−29. (d) Teets, T. S.; Lutterman, D. A.; Nocera, D. G. *Inorg. Chem.* **2010**, *49*, 3035−3043. (e) Teets, T. S.; Neumann, M. P.; Nocera, D. G. *Chem. Commun.* **2011**, *47*, 1485−1487. (f) Teets, T. S.; Cook, T. R.; McCarthy, B. D.; Nocera, D. G. *Inorg. Chem.* **2011**, *50*, 5223−5233. (g) Cook, T. R.; McCarthy, B. D.; Lutterman, D. A.; Nocera, D. G. *Inorg. Chem.* **2012**, *51*, 5152−5163.

(5) Cook, T. R.; Esswein, A. J.; Nocera, D. G. *J. Am. Chem. Soc.* **2007**, *129*, 10094−10095.

(6) Wade, C. R.; Gabbaï, F. P. *Angew. Chem., Int. Ed.* **2011**, *50*, 7369−7372.

(7) Gysling, H. J.; Luss, H. R. *Organometallics* **1984**, *3*, 596−598.

(8) (a) Pyykkö, P.; Atsumi, M. *Chem.—Eur. J.* **2009**, *15*, 186−197. (b) Cordero, B.; Gomez, V.; Platero-Prats, A. E.; Reves, M.; Echeverria, J.; Cremades, E.; Barragan, F.; Alvarez, S. *Dalton Trans.* **2008**, 2832−2838.

(9) (a) The Te−Pt bond of complexes $[\mathbf{1}]^+$, **2**, and $[\mathbf{3}]^+$ are polar and could be described using the dative formalism. However, because of the formal oxidation state or d-electron count ambiguity that the dative formalism sometimes engenders (for example, see refs 9b and c), we have chosen to describe the Te−Pt bonding in these complexes using resonance structures. In the case of **4**, the Te−Pt bond is covalent such that the compound can be properly described on the basis of a single resonance structure. (b) Hill, A. F. *Organometallics* **2006**, *25*, 4741−4743. (c) Parkin, G. *Organometallics* **2006**, *25*, 4744−4747.

(10) (a) Oberhauser, W.; Bachmann, C.; Stampfl, T.; Brüggeller, P. *Inorg. Chim. Acta* **1997**, *256*, 223−234. (b) Hope, E. G.; Levason, W.; Powell, N. A. *Inorg. Chim. Acta* **1986**, *115*, 187−192. (c) Oberhauser, W.; Stampfl, T.; Bachmann, C.; Haid, R.; Langes, C.; Kopacka, H.; Ongania, K.-H.; Brüggeller, P. *Polyhedron* **2000**, *19*, 913−923.

(11) Hope, E. G.; Levason, W. *Coord. Chem. Rev.* **1993**, *122*, 109−170.

(12) Alcock, N. W.; Harrison, W. D. *J. Chem. Soc., Dalton Trans.* **1982**, 251−255.

(13) (a) Ebsworth, E. A. V.; Holloway, J. H.; Watson, P. G. *J. Chem. Soc., Chem. Commun.* **1991**, 1443−1444. (b) Eveland, J. R.; Whitmire, K. H. *Angew. Chem., Int. Ed.* **1996**, *35*, 741−743. (c) Dyson, P. J.; Hill, A. F.; Hulkes, A. G.; White, A. J. P.; Williams, D. J. *Angew. Chem., Int. Ed.* **1999**, *38*, 512−514. (d) Torubaev, Y.; Pasynskii, A.; Mathur, P. *J. Organomet. Chem.* **2009**, *694*, 1781−1785. (e) Torubaev, Y. V.; Pasynskii, A. A.; Galustyan, A. R.; Mathur, P. *Russ. J. Coord. Chem.* **2009**, *35*, 1−5. (f) Torubaev, Y.; Pavlova, A.; Pasynskii, A. *Russ. J. Coord. Chem.* **2012**, *38*, 219−223. (g) Torubaev, Y.; Pasynskii, A.; Mathur, P. *Coord. Chem. Rev.* **2012**, *256*, 709−721.

(14) (a) Murray, S. G.; Hartley, F. R. *Chem. Rev.* **1981**, *81*, 365−414. (b) Gysling, H. J. *Coord. Chem. Rev.* **1982**, *42*, 133−244. (c) Singh, A. K.; Sharma, S. *Coord. Chem. Rev.* **2000**, *209*, 49−98. (d) Singh, A. K. *Focus Organomet. Chem. Res.* **2005**, 79−109.

(15) Janzen, M. C.; Jennings, M. C.; Puddephatt, R. J. *Inorg. Chem.* **2003**, *42*, 4553−4558.

(16) Frisch, M. J.; Trucks, G. W.; Schlegel, H. B.; Scuseria, G. E.; Robb, M. A.; Cheeseman, J. R.; Scalmani, G.; Barone, V.; Mennucci, B.; Petersson, G. A.; Nakatsuji, H.; Caricato, M.; Li, X.; Hratchian, H. P.; Izmaylov, A. F.; Bloino, J.; Zheng, G.; Sonnenberg, J. L.; Hada, M.; Ehara, M.; Toyota, K.; Fukuda, R.; Hasegawa, J.; Ishida, M.; Nakajima, T.; Honda, Y.; Kitao, O.; Nakai, H.; Vreven, T.; Montgomery, J., J. A.; ; Peralta, J. E.; Ogliaro, F.; Bearpark, M.; Heyd, J. J.; Brothers, E.; Kudin, K. N.; Staroverov, V. N.; Kobayashi, R.; Normand, J.; Raghavachari, K.; Rendell, A.; Burant, J. C.; Iyengar, S. S.; Tomasi, J.; Cossi, M.; Rega, N.; Millam, J. M.; Klene, M.; Knox, J. E.; Cross, J. B.; Bakken, V.; Adamo, C.; Jaramillo, J.; Gomperts, R.; Stratmann, R. E.; Yazyev, O.; Austin, A. J.; Cammi, R.; Pomelli, C.; Ochterski, J. W.; Martin, R. L.; Morokuma, K.; Zakrzewski, V. G.; Voth, G. A.; Salvador, P.; Dannenberg, J. J.; Dapprich, S.; Daniels, A. D.; Farkas, Ö.; Foresman, J. B.; Ortiz, J. V.; Cioslowski, J.; Fox, D. J. *Gaussian 09*, Revision B.01; Gaussian, Inc.: Wallingford, CT, 2009.

(17) (a) Perdew, J. P. *Phys. Rev. B* **1986**, *33*, 8822−8824. (b) Becke, A. D. *Phys. Rev. A* **1988**, *38*, 3098−3100.

(18) (a) Figgen, D.; Peterson, K. A.; Dolg, M.; Stoll, H. *J. Chem. Phys.* **2009**, *130*, 164108−164112. (b) Peterson, K. A.; Figgen, D.; Goll, E.; Stoll, H.; Dolg, M. *J. Chem. Phys.* **2003**, *119*, 11113−11123.

(19) For other redox processes involving atrane complexes with Metal→Lewis acid interactions, see: (a) Harman, W. H.; Peters, J. C. *J. Am. Chem. Soc.* **2012**, *134*, 5080−5082. (b) Brendler, E.; Wächtler, E.; Heine, T.; Zhechkov, L.; Langer, T.; Pöttgen, R.; Hill, A. F.; Wagler, J. *Angew. Chem., Int. Ed.* **2011**, *50*, 4696−4700. (c) Moret, M. E.; Peters, J. C. *Angew. Chem., Int. Ed.* **2011**, *50*, 2063−2067. (d) Crossley, I. R.; Hill, A. F. *Organometallics* **2004**, *23*, 5656−5658. (e) Figueroa, J. S.; Melnick, J. G.; Parkin, G. *Inorg. Chem.* **2006**, *45*, 7056−7058. (f) Crossley, I. R.; Hill, A. F.; Willis, A. C. *Organometallics* **2008**, *27*, 312−315. (g) Pang, K. L.; Tanski, J. M.; Parkin, G. *Chem. Commun.* **2008**, 1008−1010. (h) Krogman, J. P.; Foxman, B. M.; Thomas, C. M. *J. Am. Chem. Soc.* **2011**, *133*, 14582−14585.

(20) (a) Fontaine, F. G.; Boudreau, J.; Thibault, M. H. *Eur. J. Inorg. Chem.* **2008**, 5439−5454. (b) Braunschweig, H.; Dewhurst, R. D.; Schneider, A. *Chem. Rev.* **2010**, *110*, 3924−3957. (c) Bouhadir, G.; Amgoune, A.; Bourissou, D. *Adv. Organomet. Chem.* **2010**, *58*, 1−107. (d) Amgoune, A.; Bourissou, D. *Chem. Commun.* **2011**, *47*, 859−871. (e) Lin, T.-P.; Wade, C. R.; Pérez, L. M.; Gabbaï, F. P. *Angew. Chem., Int. Ed.* **2010**, *49*, 6357−6360. (f) Wade, C. R.; Lin, T.-P.; Nelson, R. C.; Mader, E. A.; Miller, J. T.; Gabbaï, F. P. *J. Am. Chem. Soc.* **2011**, *133*, 8948−8955. (g) Lin, T.-P.; Ke, I.-S.; Gabbaï, F. P. *Angew. Chem., Int. Ed.* **2012**, *51*, 4985−4988. (h) Wade, C. R.; Ke, I.-S.; Gabbaï, F. P. *Angew. Chem., Int. Ed.* **2012**, *51*, 478−481. (i) Lin, T.-P.; Nelson, R. C.; Wu, T.; Miller, J. T.; Gabbaï, F. P. *Chem. Sci.* **2012**, *3*, 1128−1136. (j) Rudd, P. A.; Liu, S.; Gagliardi, L.; Young, V. G.; Lu, C. C. *J. Am. Chem. Soc.* **2011**, *133*, 20724−20727.

(21) Liaw, W.-F.; Chiou, S.-J.; Lee, G.-H.; Peng, S.-M. *Inorg. Chem.* **1998**, *37*, 1131−1134.

(22) Marenich, A. V.; Cramer, C. J.; Truhlar, D. G. *J. Phys. Chem. B* **2009**, *113*, 6378−6396.

(23) (a) Hatchard, C. G.; Parker, C. A. *Proc. R. Soc. London, Ser. A* **1956**, *235*, 518−536. (b) Parker, C. A. *Proc. R. Soc. London, Ser. A* **1953**, *220*, 104−116. (c) Kuhn, H. J.; Braslavsky, S. E.; Schmidt, R. *Pure Appl. Chem.* **2004**, *76*, 2105−2146.

(24) Minoura, M.; Sagami, T.; Akiba, K.-y. *Organometallics* **2001**, *20*, 2437−2439.

(25) Minoura, M.; Sagami, T.; Akiba, K.-y.; Modrakowski, C.; Sudau, A.; Seppelt, K.; Wallenhauer, S. *Angew. Chem., Int. Ed.* **1996**, *35*, 2660−2662.
(26) Klapötke, T. M.; Krumm, B.; Polborn, K.; Schwab, I. *J. Am. Chem. Soc.* **2004**, *126*, 14166−14175.
(27) Herntrich, T.; Merzweiler, K. *Z. Anorg. Allg. Chem.* **2010**, *636*, 803−807.
(28) De Crisci, A. G.; Lough, A. J.; Multani, K.; Fekl, U. *Organometallics* **2008**, *27*, 1765−1779.
(29) Zhao, X.-F.; Zhang, C. *Synthesis* **2007**, 551−557.
(30) Glendening, E. D.; Badenhoop, J. K.; Reed, A. E.; Carpenter, J. E.; Bohmann, J. A.; Morales, C. M.; Weinhold, F. *NBO 5.9*; Theoretical Chemistry Institute, University of Wisconsin, Madison, WI, 2011.
(31) (a) Hall, M. B.; Fenske, R. F. *Inorg. Chem.* **1972**, *11*, 768−775. (b) Manson, J.; Webster, C. E.; Pérez, L. M.; Hall, M. B., http://www.chem.tamu.edu/jimp2/index.html.